Electronic compensation for nonideal spatial light modulator characteristics

David M. Budgett
University of Sussex
School of Engineering
Falmer
Brighton BN1 9QT
United Kingdom
E-mail: d.m.budgett@sussex.ac.uk

James H. Sharp
University of Glasgow
Department of Mechanical Engineering
Glasgow G12 8QQ
United Kingdom
E-mail: j.sharp@mech.gla.ac.uk

Pei C. Tang
National Chiao-Tung University
Department of Control Engineering
Hsin-Chu
Taiwan

Rupert C. D. Young, MEMBER SPIE
University of Sussex
School of Engineering
Falmer
Brighton BN1 9QT
United Kingdom
E-mail: r.c.d.young@sussex.ac.uk

Brian F. Scott
University of Glasgow
Department of Mechanical Engineering
Glasgow G12 8QQ
United Kingdom
E-mail: b.scott@mech.gla.ac.uk

Christopher R. Chatwin
University of Sussex
School of Engineering
Falmer
Brighton BN1 9QT
United Kingdom
E-mail: c.r.chatwin@sussex.ac.uk

Abstract. Compensation for spatial light modulator device imperfections can be achieved using digital electronics. Optical computing applications, requiring accurate phase or amplitude modulation, can then make use of low-cost, enhanced devices. Using electronic compensation, corrections can be made for a nonsquare aspect ratio in the aperture window and a nonlinear phase response—which may also be nonuniform over the aperture. The corrections for these imperfections are implemented using low-cost field programmable gate arrays. This technology enables real-time compensation and is easily adapted to suit a wide range of display devices. The performance enhancement is demonstrated using a popular Seiko-Epson liquid crystal television display operating as a phase modulating spatial light modulator. These developments greatly extend the utility of readily available, inexpensive, spatial light modulators. © *2000 Society of Photo-Optical Instrumentation Engineers.*
[S0091-3286(00)02509-5]

1 Introduction

Liquid crystal spatial light modulators have applications in optical data processing including optical computing systems,[1] optical correlators,[2] and computer-generated holograms.[3]

Low-cost spatial light modulators can be obtained from commercial video projectors. These devices have been designed for amplitude modulation, but have also been shown to be capable of providing 2π, or greater, phase modulation.[4–8] The nonideal response of these devices has been documented.[9,10] Phase errors resulting from inadequate optical flatness may be compensated by immersing the screen in a liquid gate.[9] Coding a phase-correcting pattern into the images to be displayed can also improve the phase response. This has been performed previously using off-line image manipulation.[10] The electronics described here is capable of performing corrections in real time. It therefore enables low cost SLMs to be used for applications where optical computing is most suited, that is, high-speed, real-time processing.

An application that illustrates a demanding application for an SLM is a hybrid optical/digital correlator system.[11] This system is capable of processing 3000 correlations/s. It exploits the Fourier processing capabilities of a lens to rap-
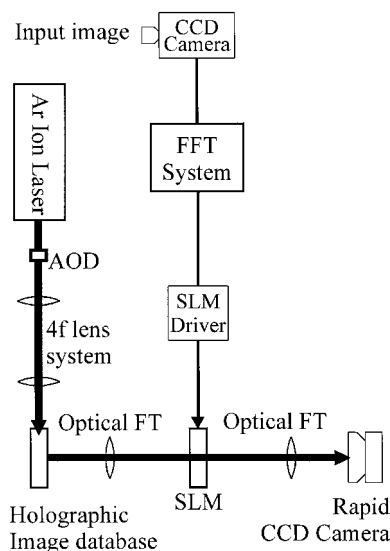
Fig. 1 Hybrid optical/digital correlator system. Optical arm modulates laser beam with rapid random access holographic memory. Single database image selected using acousto-optic deflector. Digital arm introduces phase of fast Fourier transform of input scene using an SLM. Following an optical inverse Fourier transform, the correlation plane processing ouputs a match between input and each database image. System operates at 3000 frames/s.

Fig. 2 Physical aspect ratio of LCTV pixels from Seiko-Epson VPS100 projector. All dimensions are in micrometers.

idly compute the correlation between a video input source and a high-speed randomly access image database stored in a holographic memory. The system overview is given in Fig. 1. The scene containing the object to be identified is captured by a CCD camera, the real-time Fourier transform is computed digitally,[12] and the phase of the Fourier transform displayed on a phase modulating spatial light modulator. The second, and fastest, arm of the correlator reconstructs images from a holographic database which is accessed by controlling the angular deflection of an argon ion laser beam.[13] Phase images are displayed at a rate of 25 per second. For each phase image, the database is searched by deflecting the beam using an acousto-optic deflector. The correlation output is captured and analyzed at a rate of 3000 frames/s by digital logic implemented in programmable gate arrays.[14] Output data provides information of the identity, orientation and location of an object.

The role of the spatial light modulator in this system is to accurately encode the phase image of the fast Fourier transform (FFT) of the input scene. For this task to succeed, the FFT phase image must be accurately represented by the SLM to match the spatial frequencies generated by the optical Fourier transform of the database image. The display of the FFT phase image on the SLM must be implemented at full video rates, i.e., 25 frames/s.

A Seiko-Epson liquid crystal television (LCTV) was selected for this task because it has an aperture window 320 $\times$ 264 pixels in size, and had been shown to be capable of producing greater than 2π phase modulation. To achieve this modulation depth, the device is driven with bias voltages outside its normal operating range and it has three undesirable characteristics that required correction before its use as a phase-modulating SLM. Whereas a video projector sources will convey an image with a 4:3 aspect ratio, it is desirable that the resulting image from an FFT process
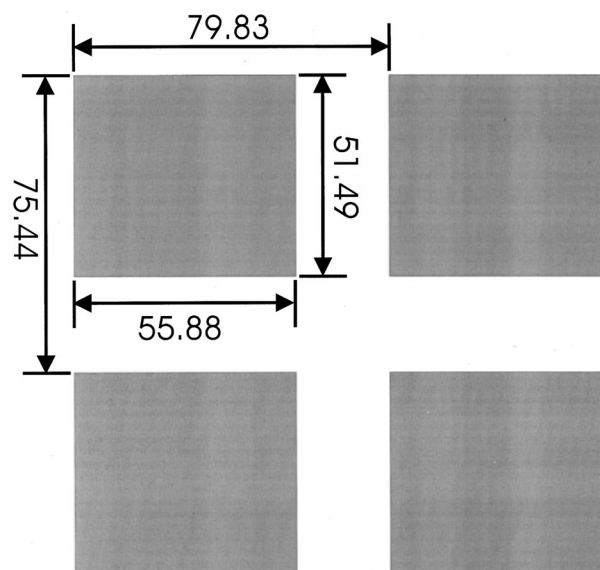
has a 1:1 aspect ratio. A second problematic characteristic is the nonlinear operating characteristic relating applied voltage to induced phase modulation. Finally, when testing the phase modulation characteristics of the Seiko-Epson LCTV, the voltage levels required to achieve a given modulation depth in one region of the aperture could be very different from those required to achieve the same modulation depth in another region. This has been termed an inhomogeneous response.

All of the undesirable characteristics described can be corrected, at video frame rates, using digital logic to (1) alter timing parameters and (2) remap linear phase values to nonlinear applied pixel voltages appropriate for each region of the SLM aperture.

2 Electronic Correction for Aspect Ratio

The image from the FFT digital processing system has a square aspect ratio, and the distribution of the spatial frequencies in the x and y directions are uniform. The SLM device has a nonsquare pixel aspect ratio, and so the Fourier phase image requires scaling to produce a square aspect ratio spectrum in the aperture of the SLM.

The dimensions of the frame buffer image is 512 $\times$ 512. The maximum number of vertical lines available on the SLM device is 264. Mapping 512 vertical pixels to 256 vertical pixels can be done easily by excluding 256 lines. For space domain images, the most appropriate method is usually dropping every alternate line. For frequency domain images, it may be more appropriate to display a 256 $\times$ 256 window from the center of the image (thus retaining all low-frequency samples and eliminating only high frequencies). In this case, the first and last 128 vertical lines of a 512-line image are dropped.

The physical dimensions of the LCTV aperture (shown in Fig. 2) determine the required image scaling for correcting the aspect ratio. The display of 256 vertical pixels will occupy a physical distance of 19.31 mm. To obtain a square
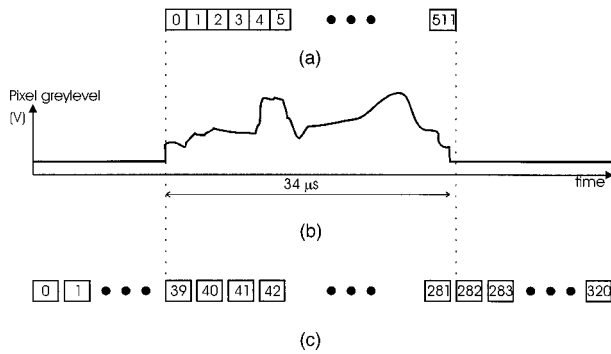
Fig. 3 Aspect ratio correction: (a) line of image data represented by 512-pixel gray levels in a frame buffer memory; (b) data used to construct a 34-μs portion of an analog voltage signal, a pixel gray-level value of zero is added to each side of image data; (c) the analog sample is resampled within the LCTV device to derive 320 horizontal pixel values.

aspect ratio, the horizontal extent of each line should also be 19.31 mm; this corresponds to 241.9 LCTV pixels. The required mapping is therefore 512→242.

Horizontal image scaling can be achieved through adjustment of the LCTV pixel clock frequency used to sample the analog representation of the image data. Conventional video transmission systems (e.g. CCIR or RS-170) use a single wire to carry an analog voltage signal, which represents the gray levels in an image (synchronization signals are also encoded into the signal). The pixel values stored in an image framebuffer are converted to an analog signal of approximately 52 μs duration per line. A pixelated display device will sample this analog signal at a rate that determines how the 52 μs of data is distributed over the available horizontal pixels. The device pixels and sample rate will determine the aspect ratio of the displayed image.

The Seiko-Epson device uses a similar video transmission system. The framebuffer generates an analog signal, as illustrated in Fig. 3. The pixel clock onboard the framebuffer is operating at 15 MHz and so 512 pixels will therefore be represented by a 34-μs portion of the analog signal. To map this data to 242 LCTV pixels, the SLM driver implements a pixel clock of 709 kHz. From the total 320 horizontal pixels, 39 pixels are available for each margin. The duration of each margin is therefore 5.5 μs, which gives the total horizontal line time of 45 μs.

Unlike conventional video systems, the Seiko-Epson device has separate inputs to control the pixel sampling rate and horizontal and vertical synchronization. Correcting the aspect ratio is therefore simplified since it requires only digital logic to produce the correct clock frequency. The digital logic was implemented using a XiLinx 3130 programmable gate array. This device is low cost and easily reconfigured for any other desired aspect ratio correction.

The aspect ratio with and without correction is shown in Fig. 4. Using the scaling techniques presented here, a live video source can be displayed with the correct aspect ratio.

Compensation for aspect ratio could be attempted by optical means, for example, by the use of a cylindrical lens. However, any advantage gained is likely to be negated by the associated phase distortion unless a carefully designed multielement lens system is employed, which will be expensive.
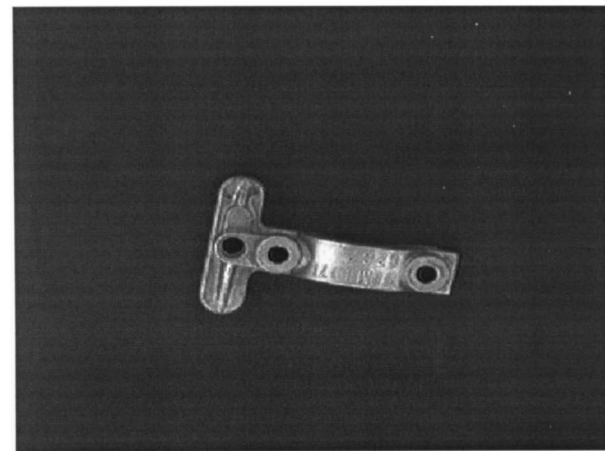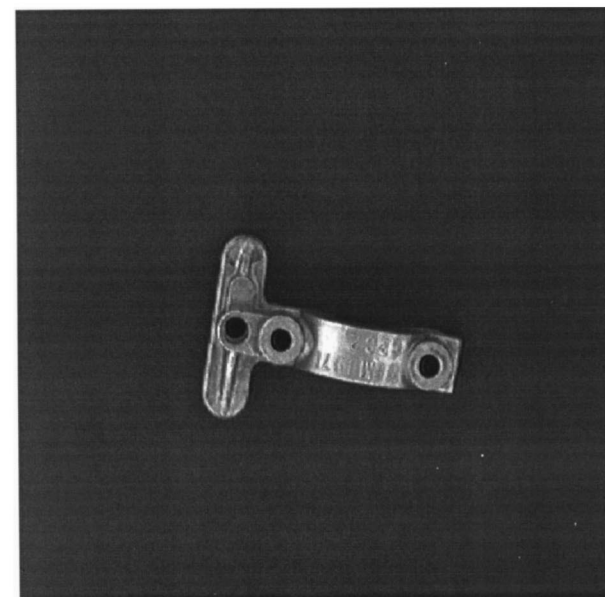
Fig. 4 Corrected aspect ratio (a) without compensation image displayed with 4:3 aspect ratio and (b) with compensation, data image correctly displayed with 1:1 aspect ratio.

3 Electronic Correction for Nonlinear Response

A linear change in the applied analog voltage to an LCTV pixel does not produce a linear change in phase modulation. To overcome this problem, a translation (or mapping) from the required linear phase modulation to appropriate nonlinear applied voltage is required.

A phase image from a digital FFT system was represented by 256 gray levels. Using gray-level 128 as a zero phase reference point, a gray level of 0 represents a $-\pi$ phase shift, and gray level of 255 a $+\pi$ phase shift. The relationship between gray level and digital phase modulation is linear.

In a conventional video signal, the voltage amplitudes for representing gray levels 0 and 255 are approximately 0 and 1 V, respectively. The video signal for driving the Seiko-Epson LCTV follows the same principle of mapping gray levels between two voltage levels but is complicated
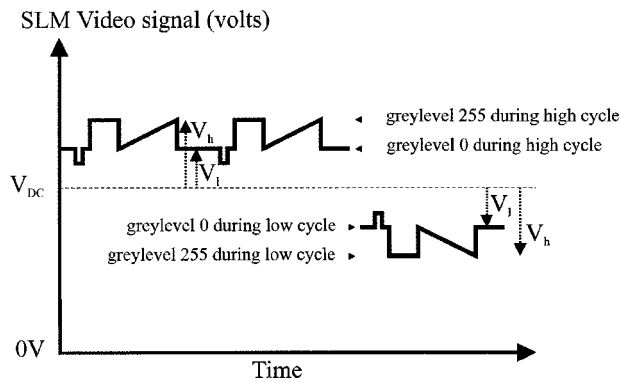
Fig. 5 Analog video signal showing dc bias and gray-level modulation voltages.

Fig. 6 Fringe patterns showing phase modulation of LCTV using a Mach-Zehnder interferometer: top half driven at 2.77 Volts and (a) lower half at 2.50 V, (b) lower half at 2.77 V, and (c) lower half at 3.22 V.

by the need to maintain a positive signal average at a fixed level of V_{dc} (typically 5 V), as shown in Fig. 5. To maintain this average, the analog signal first modulates the pixel data with a positive bias and then repeats the pixel data with a negative bias. Of greatest significance in Fig. 5 are the voltage levels labeled V_1 and V_h. These values represent the limits of the voltage range that can be produced in response to the framebuffer outputting a value at gray level 0 and gray level 255. The selection of these values (and intermediate phase response) requires the measurement of phase modulation as a function of applied voltage.

The phase shift was measured using a Mach-Zehnder interferometer: the SLM was placed in one arm of the interferometer and, for a uniform phase shift, a series of vertical interference fringes was observed from the output of the interferometer. By driving the first 128 LCTV rows with a voltage different from the second 128 rows, a shift in fringe pattern occurred at the boundary of the two regions. The amount of shift in relative fringe positions over the region boundary quantifies the difference in phase modulation between the two regions. A relative shift of 2π will again align the fringes across the region boundary. The fringe patterns that represent $-\pi$, 0, and $+\pi$ phase shifts and their corresponding voltage levels are shown in Fig. 6.

Fractional phase shifts are more easily quantified using fewer interference fringes. The nonlinear phase modulation response to a linear applied voltage for a red channel Seiko-Epson LCTV is given in Fig. 7; this is consistent with the response observed by others.[15] Approximating the response with a linear function will produce maximum errors in phase modulation in the order of 10%. To display the FFT phase data more accurately, the linear gray-level values should be remapped to a new set of gray-level values that will produce the voltage that produces the desired phase modulation.

The nonlinear response can be corrected in realtime by the use of a digital look-up table (LUT). This requires an 8-bit static random access memory (SRAM) with 256 locations. The first location contains the data zero, the ith location contains the gray level that will produce a phase shift of $i/256 \times 2\pi$, as observed from Fig. 7. The output of the framebuffer memory is used to address the SRAM, and the output of the SRAM is used to generate the analog video signal. This method remaps the linear phase data to a nonlinear response defined in the SRAM in real time. Follow-
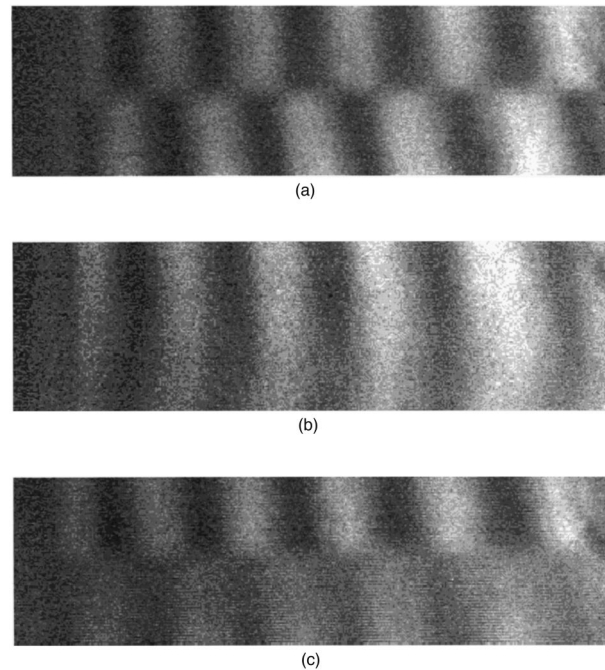
ing implementation of the LUT, the fringe patterns shown in Fig. 6 are produced by displaying an image whose top half is set to gray level 128, and bottom half set to 0, 128, and 256 for Figs. 6(a), 6(b), and 6(c), respectively.

Corrections for different nonlinear responses for devices from the same Seiko-Epson family are derived using the measurements from the Mach-Zehnder interferometer and stored in a configuration file. To use a particular device, the contents of the appropriate configuration file is read to obtain the device specific LUT corrections.

The phase quantization levels are reduced using the LUT scheme. The phase image contains 256 levels of phase data. The LUT will map each of these levels to a value
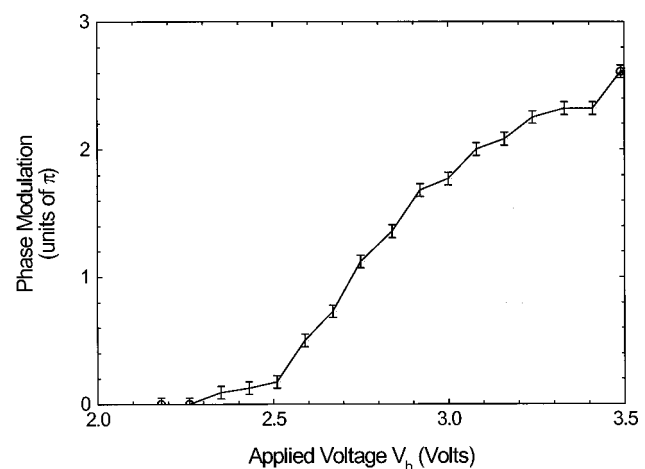

Fig. 7 Plot showing nonlinear phase modulation response to linear increase of V_h (V_1 constant at 2.18 V, $V_{dc}=5.09$ V).
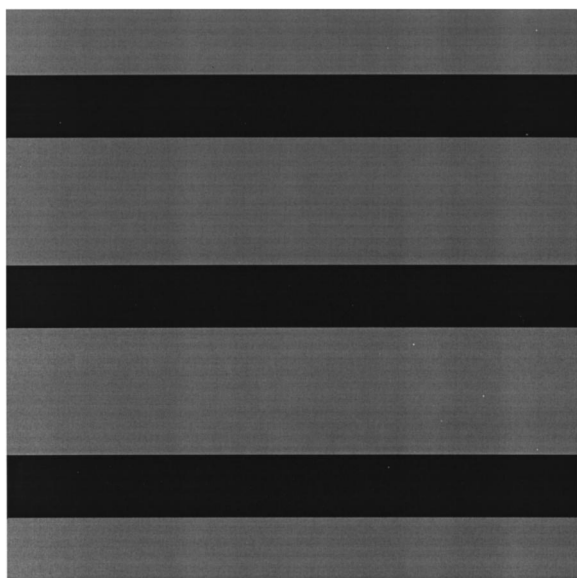
Fig. 8 Test image for the purpose of establishing uniformity of phase modulation over device aperture. At each gray (pixel intensity 128) and black (pixel intensity 0) boundary, a π phase shift should result.

Fig. 9 Nonhomogeneous phase response under uniform driving conditions. Test image of Fig. 8 is displayed using the same driving voltages over the device aperture. The boundary between the top bar and the background shows a shift of almost 2π, the middle bar boundary is in the region of π (as desired), and the bottom bar introduces only a fractional shift.

representing a voltage between V_1 and V_h, which covers the voltage range required over the entire aperture. The range V_h to V_1 is represented by only 256 possible levels, and the 256 phase levels occupy only part of this range—producing a many to one mapping. Based on simulations of the effect of phase quantization on the correlator output plane,[16] the reduction in the number of discrete phase levels available will not degrade the discrimination capability of the hybrid optical/digital correlator system described here. If this was important for other applications, then the reduction in phase levels could be eliminated by using a higher resolution LUT memory. For example, if the V_h to V_1 range was represented by 16 bits, it is highly probable that the 256 phase values will map onto 256 unique values for input to the digital-to-analog (D/A) converter.

4 Electronic Correction for Inhomogeneous Response over the Device Aperture

The values for V_1 and V_h and the LUT contents derived in the preceding section were based on the behavior of the interference fringes at the vertical center of the aperture. It was observed that different phase modulation was attained using identical voltages at different locations in the aperture.

The behavior of the fringe pattern to a test image (Fig. 8) consisting of three bars on a uniform background is shown in Fig. 9. The upper third has achieved a 2π shift, the middle section π, and the lower section almost no phase shift in comparison to the background level.

The device is designed to operate as an amplitude modulating device. By biasing the device with a higher V_h than that supplied by the commercial device driver, a 2π phase modulation was achieved. It would seem that a consequence of driving the device outside its design specifications could be a degradation in spatial response uniformity.
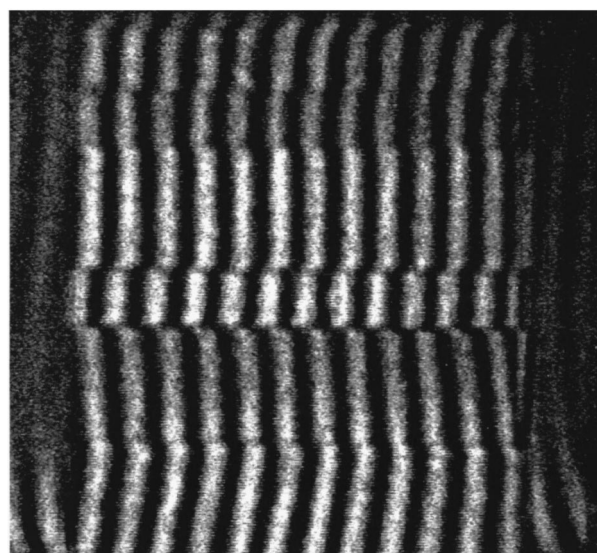
Given the ease with which a LUT can be implemented to correct for nonlinear response, one solution to the nonuniform behavior is to divide the aperture into a number of regions, e.g., eight, and implement a different LUT for each region. The physical realization of this approach is discussed in the next section.

5 LCTV Driver Electronics

The unique architecture of the digital electronic system designed for driving LCTV devices given in Fig. 10, provides real-time compensation for aspect ratio and nonuniform, nonlinear phase response specific to the attached SLM device.

A 512×512 8-bit image representing linear phase data is stored in two image memories, one receives the incoming 512×512 image data (either from the FFT system or via a CCIR analog input interface), while the other supplies the previously captured data for display on the SLM. These memories alternate roles every 40 ms and maintain a throughput rate of 25 frames/s.
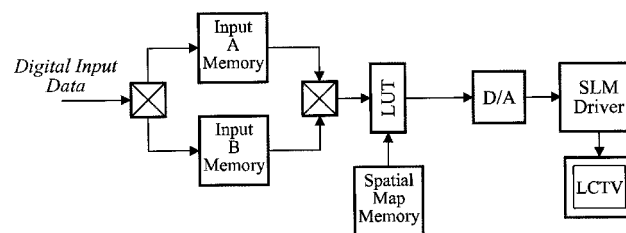

Fig. 10 SLM electronics for correction of nonuniform, nonlinear response. Input memories *A* and *B* hold the linear 512×512 gray-level phase image. Spatial map memory selects which LUT is used for each pixel. Finally, the appropriate voltage is generated by the D/A converter.

Fig. 11 Contents of spatial map memory to divide LCTV aperture into three regions. All pixels in the top left region will use LUT 0 for remapping gray-level values, pixels in the middle region will use LUT 1, etc. The shape and size of each region is arbitrary.
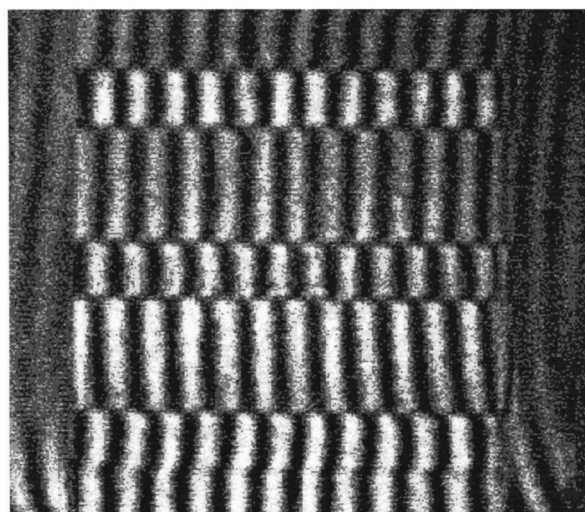

Fig. 12 Corrected phase response showing three bars of gray level 128 on a background of gray level 0. The π phase shift is achieved over the majority of the aperture. A region at the bottom of the device could not attain a π phase shift that was consistent with both a 0 and a 255 gray-level background—the best compromise is shown here.

A 256×256 LUT memory contains a maximum of 256 different lookup tables. Each lookup table specifies a conversion for a 0 to 255 gray level linear range to a new range that will output a voltage (between V_1 and V_h) that corresponds to the required phase modulation. The conversion will depend on which region on the LCTV aperture that the pixel is mapped to. A maximum of 256 different regions can be specified.

A 512×512 spatial map memory specifies which LUT should be used for each pixel. If the LCTV has been divided into three equal-sized horizontal bands, then the data values in this memory should be set as shown in Fig. 11. Any spatial division can be implemented. Each pixel is assigned to one of a possible 256 LUTs. A common counter addresses both the spatial map memory and image memory. Output data from the spatial map memory addresses the high byte of the LUT memory address (and selects the appropriate LUT), output data from the image memory addresses the low byte of the LUT memory address (and selects the appropriate translation from a linear value to a nonlinear value, which will produce the desired phase shift). The output data from the LUT memory is passed into the D/A converter to formulate the analog video signal.

Implementation of all correction features is illustrated in Fig. 12. A consistent and linear phase modulation was achieved over the majority of the aperture window. The full π modulation has not been achieved below the third bar. Although up to 2π phase modulation can be achieved in this region, the location of a midrange voltage that achieves π modulation is not consistent with both a 0 and 255 background level. This type of behavior was typical for other lines in the LCTV at lower bias voltages. However, consistent operating regions could be found within the V_1 and V_h bounds for the majority of the device. It is speculated that increasing the V_h voltage could further extend the phase

modulation operating curve to include a consistent π phase shift from both 0 and 255 background levels. This was not attempted due to the possibility of damaging the SLM device.

The hardware (Fig. 13) consists primarily of memory and PGAs mounted on a six-layer printed circuit board. It interfaces to a PC via an ISA slot and initialization and configuration is performed using high-level windows software written in C. Data can be sourced from digital input ports (e.g., a digital FFT system), an analog video input (e.g., CCIR or PAL), or via the ISA bus for static image display—this is useful for displaying test and calibration images. Output options incorporate digital and analog capabilities. A small analog module, specific to the Seiko-Epson LCTV, is added to the core hardware to perform signal conditioning and to accommodate the peculiar biasing requirements.

The extensive use of PGAs provides great flexibility in the range of image processing functions that can be performed. In addition to image scaling, a 512×512 image can be displayed with alternate pixels dropped, or a window of data can be extracted from the full-size image. Input from interlaced video sources can be buffered and processed in real time. Timing parameters are fully programmable and accelerated display rates and image refreshing options have been tested.

6 Conclusions

The performance of low-cost SLMs can be enhanced using electronic techniques. A major advantage of this approach is the ability to perform corrections for aspect ratio and nonuniform, nonlinear phase response in realtime. Additionally, phase image corrections, which are specific to each SLM, are all encapsulated into the device driver. This removes the necessity for other digital and optical systems components to cater for specific device dependencies.
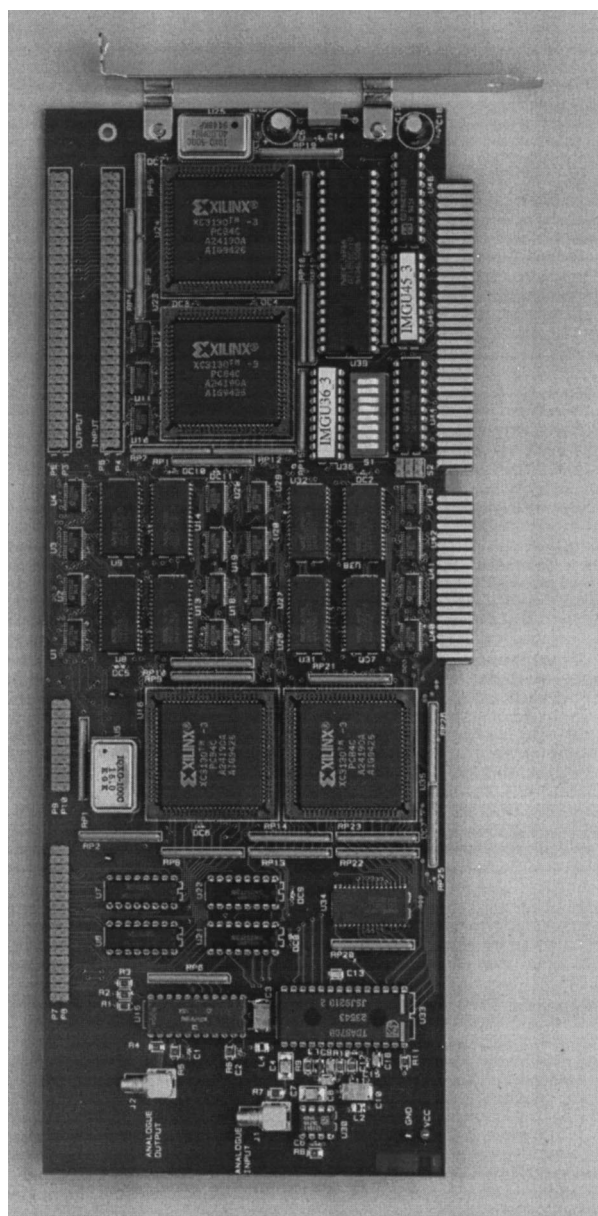

Fig. 13 Photo of hardware that compensates for LCTV imperfections in real time.

The use of programmable gate arrays and memory LUTs facilitates easy adaptation to driving a device in many modes, immediate accommodation of other devices of the same family, and rapid adaptation to other SLM families. An additional signal conditioning module may be necessary to accommodate specific biasing conditions.

Acknowledgments

References

1. Y. Ichioka, T. Iwaki, and K. Matsuoka, ''Optical information processing and beyond,'' *Proc. IEEE* **84**(5), 694–719 (1996).
2. D. A. Gregory, ''Real-time pattern recognition using a modified liquid-crystal television spatial light modulator,'' *Appl. Opt.* **25**, 467–469 (1986).
3. J. Amako and T. Sonehara, ''Computer-generated hologram using TFT active matrix liquid crystal spatial light modulator,'' *Jpn. J. Appl. Opt.* **29**(8), 1533–1535 (1990).
4. C. Soutar and K. Lu, ''Determination of the physical properties of an arbitrary twisted-nematic liquid crystal cell,'' *Opt. Eng.* **33**(8), 2704–2712 (1994).
5. K. Ohkubo and J. Ohtsubo, ''Evaluation of LCTV as a spatial light modulator,'' *Opt. Commun.* **102**, 116–124 (1993).
6. V. Laude, S. Maze, P. Chavel, and P. Refregier, ''Amplitude and phase coding measurements of a liquid crystal television,'' *Opt. Commun.* **103**(1), 33–38 (1993).
7. D. A. Gregory, T. D. Hudson, and J. C. Kirsch, ''Measurement of spatial light modulator parameters,'' *Proc. SPIE* **1297**, 176–185 (1990).
8. J. C. Kirsch, D. A. Gregory, M. W. Thile, and P. K. Jones, ''Modulation characteristics of the Epson liquid crystal television,'' *Opt. Eng.* **31**(5), 963–970 (1992).
9. A. M. Tai, ''Low-cost LCD spatial light modulator with high optical quality,'' *Appl. Opt.* **25**, 1380–1382 (1986).
10. H. M. Kim, J. W. Jeong, M. H. Kang, and S. I. Jeong, ''Phase correction of a spatial light modulator displaying a binary-only filter,'' *Appl. Opt.* **27**(20), 4167–4168 (1988).
11. D. M. Budgett, J. H. Sharp, P. C. Tang, and C. R. Chatwin, ''Implementation of a high speed optical digital correlator system,'' *Opt. Inform.*, European Optical Society Topical Digest Series, 6 2.2 (1995).
12. D. M. Budgett, J. H. Sharp, B. F. Scott, and S. Tonda, ''A hybrid correlator utilising fast Fourier transform hardware,'' presented at *12th Mtg. of the D'Etude Du Cercle D'Opto-informatique*, Paris (Oct. 1996).
13. J. H. Sharp, D. M. Budgett, C. R. Chatwin, and B. F. Scott, ''A high speed, acousto-optically addressed optical memory,'' *Appl. Opt.* **35**(14), 2399–2402 (1996).
14. D. M. Budgett, P. C. Tang, J. H. Sharp, R. K. Wang, and B. F. Scott, ''Parallel pixel processing using programmable gate arrays,'' *Electron. Lett.* **32**(17), 1557–1559 (1996).
15. A. R. Pourzand and N. Collings, ''Detailed experiments on phase modulating SLM characteristics,'' Technical Report T213-1 on International BRITE-EuRAM Project RY1-Hybrid, Doc. Ref. RY1/TR/NCH/NC&ARP950523, Con. No. BRE2-CT93-0542, DGXII-CEC-BRUSSELS, 1-14 (1995).
16. J. H. Sharp, T. G. Slack, D. M. Budgett, and B. F. Scott, ''Compact phase conjugating correlator: simulation and experimental analysis,'' *Appl. Opt.* **37**(20), 4380–4388 (1998).
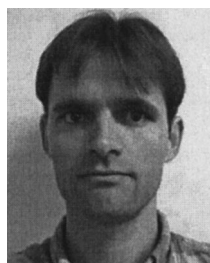
David M. Budgett graduated from Canterbury University, New Zealand, in 1989 with a first-class honors degree in electrical engineering. He furthered interests in medical technologies at Imperial College, where he received his PhD degree in 1995. He has developed novel systems for optical computing and highspeed pattern recognition at the University of Glasgow. During a 2-year lecturing position at the University of Auckland, he developed multichannel data acquisition systems. In 1999 he took up a faculty position with the School of Engineering, University of Sussex, where he is continuing research into digital systems, image processing, rapid prototyping, and microrobotics.
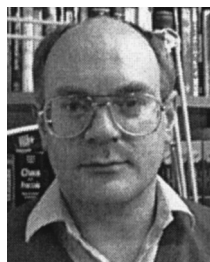
Rupert C. D. Young graduated from Glasgow University in 1984 with a degree in engineering. Until 1993 he was with the Laser and Optical Systems Engineering Research Center at Glasgow, during which time he gained wide experience in optical systems engineering and image/signal processing techniques. He received his PhD degree in 1994 for research into optical pattern recognition. In 1993 he become a senior scientific officer with the Defence Research Agency, Malvern, where he conducted research into optical processing techniques and spatial light modulator technology. In April 1995 he became a lecturer and in October 1998 a senior lecturer with the School of Engineering, University of Sussex, where he is continuing research into various aspects of optical pattern recognition, digital image processing and electro-optics system design

and applying this to a wide range of problems of industrial relevance.

Christopher R. Chatwin holds the Chair of Industrial Informatics and Manufacturing Systems (IIMS) at the University of Sussex, United Kingdom, where inter alia, he directs the IIMS Research Centre and the Laser and Photonics Systems Research Group. Before moving to Sussex, he spent 15 years with the Engineering Faculty of the University of Glasgow, Scotland, where as a reader he headed the Laser and Optical Systems Engineering Centre and the Industrial Informatics Research Group; during this period he ran a succession of major national and international interdisciplinary research programs. Prior to this he was in the automotive industry. He has published two research level books on numerical methods and hybrid optical/digital computing and more than 100 international papers focusing on optics, optical computing, signal processing, optical filtering, holography, laser materials processing, laser systems and power supply design, laser physics beam/target interactions, heat transfer, knowledge-based control systems, expert systems, computer integrated manufacture, CIM scheduling, manufacturing communication systems, computational numerical methods, genetic algorithms, maximum entropy algorithms, chaos, robotics, instrumentation, digital image processing, intelligent digital control systems and digital electronics. Professor Chatwin is on the editorial board of the international journal *Lasers in Engineering* and is editor of the RSP/Wiley book series on 'Industrial Informatics and Integrated Manufacturing Business Systems. He is a member of the institute of Electrical and Electronic Engineers, the SPIE, the European Optical Society, the Association of Industrial Laser Users, the Laser Institute of America, and the New York Academy of Sciences and a senior member of the Society of Manufacturing Engineers. He is a chartered engineer, euro-engineer, chartered physicist, and a fellow of the Institute of Electrical Engineers, the Institute of Mechanical Engineers, and the Institute of Physics.

Biographies of the other authors not available.